International Journal of Innovative Research in Engineering
Volume 7, Issue 6 (November - December 2026), PP: 106-112.
https://www.doi.org/10.59256/ijire.20260706012
www.theijire.com
ISSN No: 2582-8746

Design and Simulation of a Graphite Cleaning Robot System

Baosheng Chen[1], Mengyi Sun[2]
[1,2] *School of Intelligent Manufacturing, Zhejiang Institute of Communications, China.*

How to cite this paper:
Baosheng Chen[1], Mengyi Sun[2], "Design and Simulation of a raphite Cleaning Robot System", IJIRE-V7I6-106-112.

Copyright © 2026 by author(s) and Fifth Dimension Research Publication. This work is licensed under the Creative Commons Attribution International License (CC BY 4.0).
http://creativecommons.org/licenses/by/4.0/

Abstract: *To address the problems of high cost, low efficiency, and prominent safety hazards caused by manual chiseling for graphite cleaning at coal-charging ports in the coking industry, an automatic graphite cleaning system based on a six-axis industrial robot was designed. Considering high-temperature service conditions, a stainless-steel cleaning end-effector with air-curtain thermal insulation was designed. The system adopts an S7-1200 PLC as the main controller and realizes real-time communication with the ABB six-axis industrial robot via the PROFIBUS-DP bus, realizing the integration of rapid tool-change, furnace-cover manipulation and cleaning tasks.A virtual workstation was established in RobotStudio to plan a composite cleaning trajectory consisting of straight and inclined segments. Kinematic simulations were conducted to verify the robot's joint movements, interference, and singular configurations. Simulation results indicate that all robot joint movements remain within the permitted travel range, with no collisions, interference, or singular configurations; The net cleaning time per hole is 105 s, and the complete operation cycle is 165 s, which meets the 180-second coal-charging cycle requirement for coke ovens. This robotic cleaning system enables unmanned cleaning of coal-charging holes, reducing operation time and eliminating safety hazards.*

Key Words: *Industrial Robot; Graphite Cleaning; PROFIBUS-DP; Trajectory Planning.*

I.INTRODUCTION

In the coke production process, coal loaded into the carbonization chamber is converted into coke through high-temperature pyrolysis. The carbonization chamber must repeatedly undergo cyclic operations such as coal charging and coke discharge. During coal charging, the charging port is subjected to rapid temperature fluctuations; under the influence of repeated high- and low-temperature changes, graphite deposits gradually form on the port walls. If not removed in a timely manner, the graphite will continue to thicken and harden, reducing the effective diameter of the charging port and thereby disrupting normal coal-charging operations 1. In severe cases, it can also hinder the smooth progress of the coke-pushing process; furthermore, large graphite chunks falling into the system may result in blockage or jamming of the rotary seal valve in the dry coke quenching system, jeopardizing the stable operation of the entire coke conveying chain. Therefore, it is essential to promptly remove the graphite from the charging port.

In the coking industry both domestically and internationally, graphite removal from coal-charging ports still relies on manual chiseling, which is generally time-consuming, inefficient, and poses significant safety hazards2,3. Researchers have conducted extensive studies on graphite removal from coal-charging ports. Zhang Zhiqiang was among the first to use a scraper attached to the head of a coke-pushing rod to remove graphite; while this method yielded good results, it was only applicable to the top of the carbonization chamber and was not suitable for coal-charging ports4. Liu Juncang et al. adopted two hydraulically-driven stainless-steel ring chains with a double-helix structure for vertical cleaning of coal-charging ports; while this method prevented damage to the refractory bricks inside the ports, it was unable to remove graphite deposits at the sloped openings 5. Chen He et al. designed a chisel-hammer structure; however, when the coal-charging port was not perfectly vertical, the device would either become jammed in the port or damage it 6.

Therefore, while existing mechanical cleaning solutions can handle straight sections, they struggle to conform to the inverted-funnel-shaped beveled opening. Considering the high spatial flexibility of six-axis industrial robots, this paper proposes an operation scheme where a cleaning rod is mounted onto the end-effector of a six-axis industrial robot. The aim is to achieve integrated cleaning of both straight and beveled sections without the need for additional changeover mechanisms. The potential for interference in the motion trajectories was verified using RobotStudio software.

II. OVERALL SYSTEM DESIGN

The structure of the coke oven charging port is shown in Figure 1. Considering actual on-site conditions and technical site requirements, the graphite cleaning system must be capable of simultaneously cleaning the walls of the charging port and the inverted-funnel section of the charging port.

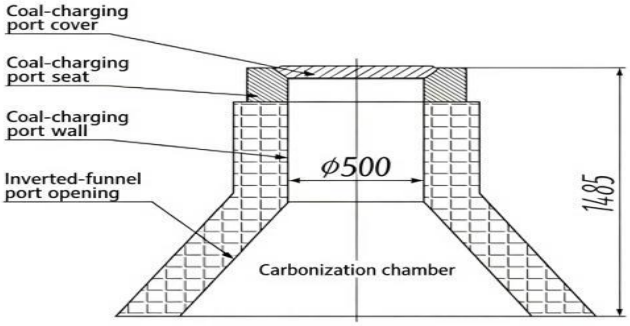


Figure 1: Schematic Diagram of the Coke Oven Coal Charging Port Structure

The cleaning rod is mounted at the end of the robot to clean both the straight and inclined sections of the charging port. When cleaning the straight section of the coal-charging port, the robot mimics the manual method of inserting and withdrawing the scraper, performing this reciprocating motion along the inner circumference of the port; when cleaning the inclined section, the robot adjusts its orientation, inserts the cleaning rod into the inclined opening, and performs scraping motions along the wall of the inclined section. The operating principle is shown in Figure 2.

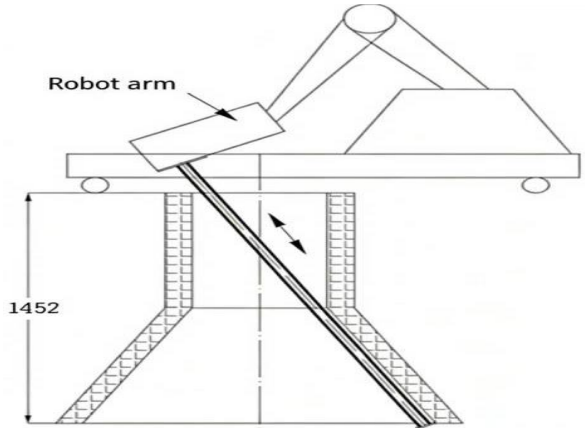


Figure 2: Schematic Diagram of the Robotic Cleaning Solution

III. STRUCTURAL DESIGN

3.1 Main Body Structural Design

The system consists of a mobile cart, a six-axis industrial robot, a quick-change assembly, a cleaning fixture, and an accompanying control system. Given the limited space at the top of the coke oven and the need to frequently switch between lid removal and cleaning operations, the system is equipped with an automatic quick-change device. This device enables the robot to rapidly switch between an electromagnetic gripper and a cleaning rod within the same workstation, effectively avoiding spatial interference issues caused by the coordination of multiple pieces of equipment.

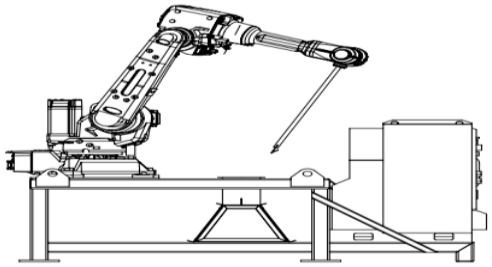


Figure 3: Robotic System Structure

3.2 Cleaning Rod Design

According to the design analysis for the graphite-cleaning scheme, the cleaning rod is a critical component of the graphite cleaning robot. The temperature inside the coal-charging port can reach 800 °C under smothered-fire conditions and up to 1000 °C under open-fire conditions; high-temperature thermal radiation can damage the robot's end-effector flange. To address this, annular air-curtain nozzles were added to the cleaning rod. Compressed air is used to form a thermal barrier that blocks the high-temperature heat waves and protects the robot's end-effector7. The structure of the cleaning rod is shown in Figure 4.

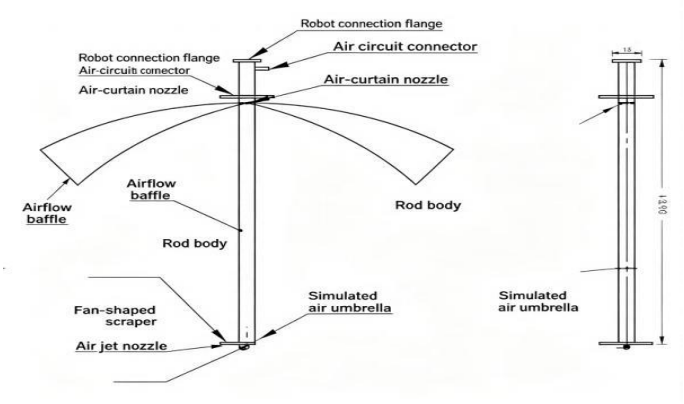


Figure 4: Structural Diagram of the Cleaning Rod

A fan-shaped scraper is located at the bottom of the rod; the robot drives this scraper to follow the inner wall of the coal-charging port, simulating manual scraping. A structural diagram of the fan-shaped scraper is shown in Figure 5.
An air nozzle is installed at the bottom of the scraper, directly facing the scraping zone, to direct compressed air

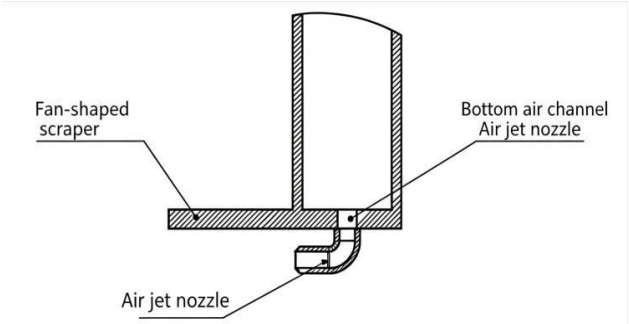


Figure 5: Sector-Shaped Scraper Structure Diagram

toward the scraping zone for graphite removal. The structural diagram of the air nozzle is shown in Figure 6.

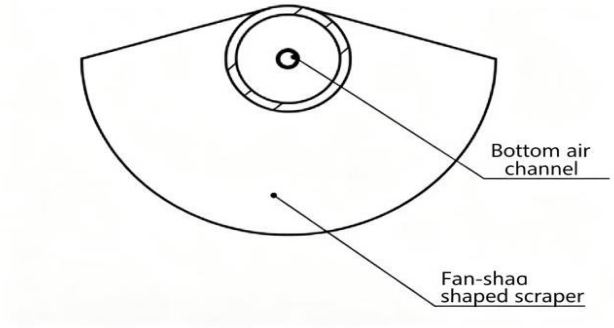


Figure 6: Air Nozzle Structure Diagram

The high-temperature oxidation resistance and high-temperature strength of the end-effector material are key design constraints. This system employs 310S austenitic heat-resistant stainless steel, which has a tensile strength (σb) ≥ 520 MPa and a yield strength ($\sigma 0.2$) ≥ 205 MPa at room temperature. It exhibits excellent oxidation resistance at temperatures below 1150 °C, satisfying the structural-stability requirements of the cleaning rod under high-temperature cyclic thermal loads8.

IV. CONTROL SYSTEM DESIGN

4.1 Hardware Implementation of the Control System

The system uses a Siemens S7-1200 PLC as its core controller, coupled with an ABB six-axis industrial robot to execute cleaning operations for straight and inclined sections. Real-time data exchange between the PLC and the robot is achieved via the PROFIBUS-DP fieldbus. Compared to Ethernet protocols, PROFIBUS-DP features a microsecond-level deterministic cycle time, which meets the requirements for real-time coordinated control of high-frequency discrete actions such as lid removal, rapid tool-change, and cleaning9. The hardware architecture of the control system is shown in Figure 7.

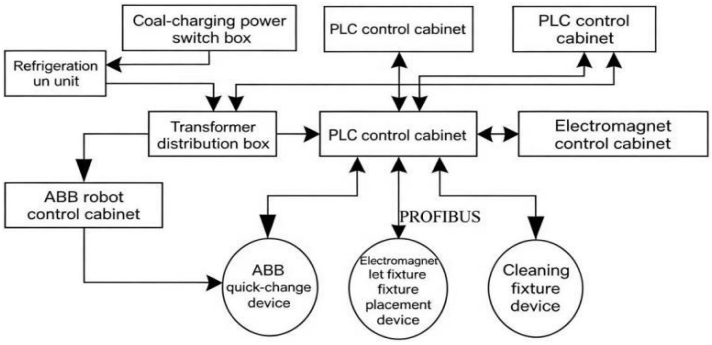


Figure 7 Control System Hardware Block Diagram

4.2 Software Implementation of the Control System

The complete sequence of the automated cleaning operation is shown in Figure 8, which includes position calibration, furnace lid opening and closing, rapid tool-change, cleaning operation, and mechanism reset.

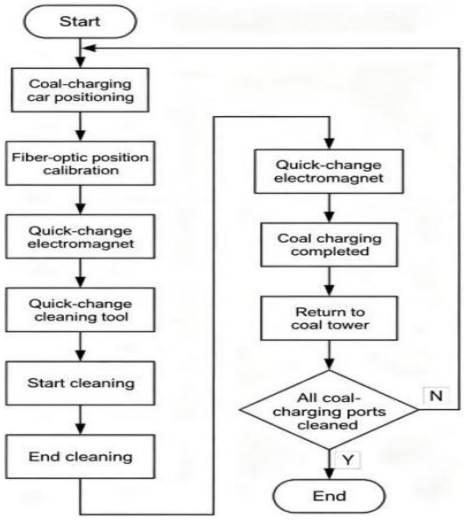


Figure 8: Graphite Cleaning Flowchart

The PLC and the robot exchange operation commands and operational status feedback via digital I/O signals (as shown in Table 1).

PLC Inputs	Robot Output	Function	PLC OUTPUT	ROBOT INPUT	Function
I200.0	DO00	Open the solenoid cylinder cover	Q200.0	DI00	Left manhole cover activated
I200.1	DO01	Open the sweeper cylinder cover	Q200.1	DI01	Right manhole cover activated
I200.2	DO02	Quick-change clamping	Q200.2	DI02	Start button
I200.3	DO03	Quick-change release	Q200.3	DI03	Stop button
I200.4	DO04	The robot is working	Q200.5	DI05	Reset
I200.5	DO05	Task completed successfully	Q200.6	DI06	Emergency stop

Table 1: PLC Input Table

The robot cleaning motions are programmed adopting a layered modular programming strategy. The main program calls three function subroutines: rDo (straight-wall scraping), rDo2 (beveled-edge wall-following cleaning), and rToHome (reset). In terms of trajectory strategy, joint motion (MoveJ) is adopted for workstation transitions to minimize non-operating time; whereas linear interpolation (MoveL) is applied for scraping motions to ensure constant contact pressure between the scraper and the furnace wall. The SingArea\Wrist instruction enables flexible adjustment of the wrist posture, effectively preventing robot kinematic lockup when traversing singular regions near the inclined section. The contents of the main program are shown in Figure 9.

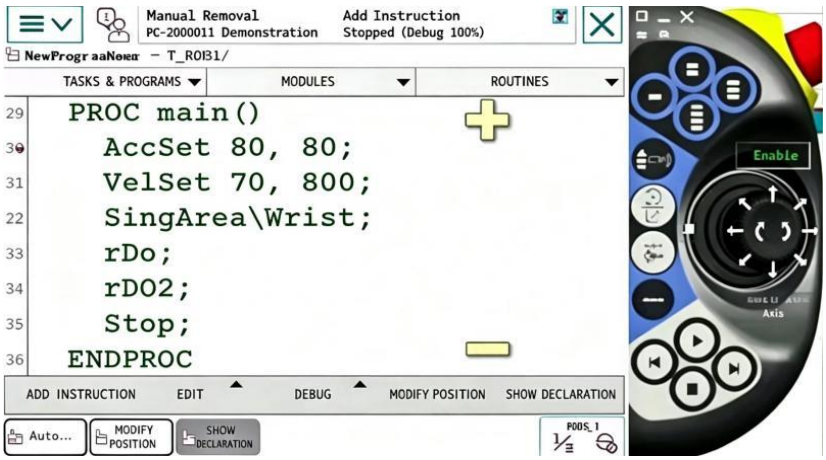


Figure 9: Main Program "main"

To realize visual monitoring and operation for the graphite-cleaning process, the HMI interface was developed using WinCC within TIA Portal V13; the human-machine interface for coal-charging port cleaning is shown in Figure 10.

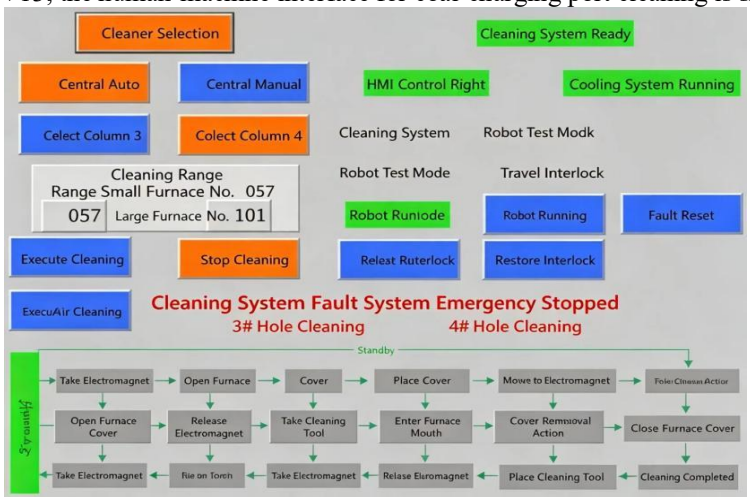


Figure 10: "Coal Charging Port Cleaning" Interface Diagram

V. SYSTEM SIMULATION AND VALIDATION

To verify the validity of the motion control program and the mechanical structure, this paper used ABB RobotStudio software to set up a virtual simulation workstation and validated the robot's motion planning.

5.1 Simulation Platform Construction

Within RobotStudio, a virtual workstation was constructed, where the ABB IRB 4600-60/2.05 robot (rated payload 60 kg, maximum reach 2.05 m, repeatability ±0.05 mm), the control cabinet, the end-of-arm tooling for cleaning, the mobile cart, and the coal-charging port model were imported. The interface of the completed simulation workstation is shown in Figure 11.

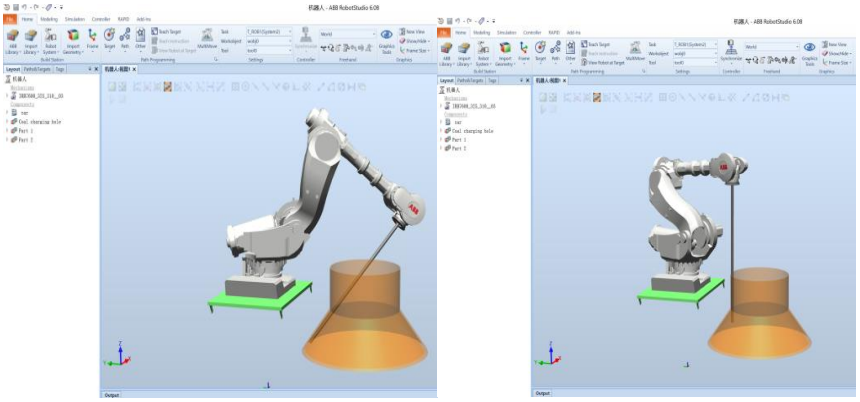


Figure 11: Straight and Inclined Sections Interface Diagram

5.2 Planning Sweeping Trajectories for Straight and Inclined Sections

Cleaning of the straight section employs a vertical reciprocating scraping strategy along the bore wall. The circumference of the bore is divided into 8 equal positions at 45° intervals; the cleaning rod is kept vertical, with its axis offset by approximately 50 mm relative to the bore axis to ensure the fan-shaped scraper adheres to the wall. The scraping stroke per position is 500 mm, matching the depth of the straight section; joint motion (MoveJ) is adopted for workstation transitions, whereas linear interpolation (MoveL) is applied for scraping motions.

For cleaning the tapered section, the end-effector's orientation must be adjusted so that the scraper moves along the tapered wall surface. Let the angle between the funnel wall and the vertical direction be α, and the depth of the straight section be h1. When the scraper is at a depth of d (d > h1), the lateral offset of the cleaning rod at the interface between the straight section and the funnel opening is $(d - h1)(\tan\theta - \tan\alpha)$; to avoid interference between the cleaning rod and the bore wall of the straight section, the condition $\theta \geq \alpha$ must be satisfied. Accordingly, the rod inclination angle θ is set to 22° (allowing a 2° margin relative to α = 20°). The wall-following stroke for a single station is 985 mm, which is also divided into 8 stations, where the rod executes reciprocating scraping along the tapered wall via the MoveL instruction. The key simulation parameters are listed in Table 2.

Parameters	Values	Parameters	Values
Total depth of the coal-charging borehole / mm	1485	Horizontal offset of the base / height above the borehole opening / mm	600 / 350
Inner diameter / depth of the straight section / mm	φ500 / 500	Number of stations on the circular track / units	8（Interval 45°）
Height of the inverted bell-mouth section / inner diameter of the outlet / mm	985 / φ1200	Angle of inclination θ of the inclined section of the rod / (°)	22
Angle between the bell-mouth wall and the vertical α / (°)	20	Insertion / repositioning speed / ($mm \cdot s^{-1}$)	240 / 500
Diameter / total length of the cleaning rod / mm	φ35 / 1950	Net cycle time per hole / complete cycle / s	105 / 165

Table 2: Simulation Parameter Table

5.3 Analysis of Kinematic Simulation Results

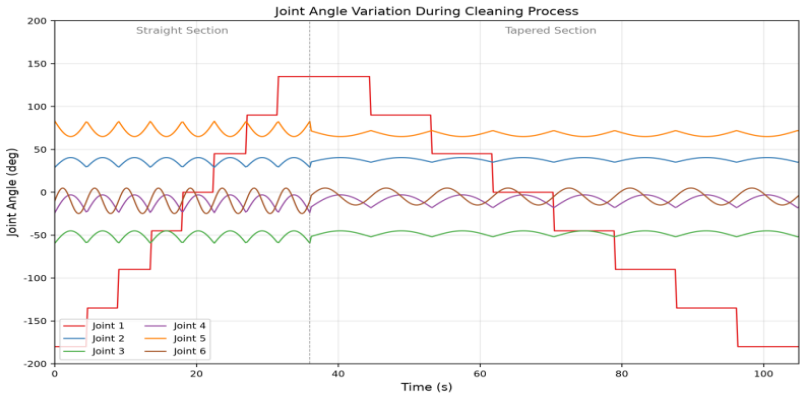


Figure 12: Joint Angle Change Curves

The angle change curves for each joint are shown in Figure 12. Joint 1 rotates in 45° increments within its working range of −180° to 135°, while the angular displacements of joints 2 through 6 are 29.0° to 40.5°, −59.5° to −45.0°, −24.0° to −3.0°, 65.0° to 83.0°, and −10.0° to 4.9°, respectively. All joints remained within their permitted range of motion throughout the entire process, and the angular displacement curves were continuous and smooth, with no abrupt changes at the transitions between straight and sloped segments.

The end-effector's pose angles and linear velocity curves are shown in Figure 13. During cleaning of the straight section, the end-effector's pose angles about the X and Y axes were both 0°; during cleaning of the inclined section, the pose angle about the X axis remained stable at −22°, consistent with the theoretical inclination angle θ, while the pose angle about the Y axis remained at 0° throughout, which indicates no extra lateral deviation during wall-following motion. The peak repositioning speed is approximately 500 mm/s, while the cutting segment maintains a constant speed of approximately 240 mm/s; the speed curve exhibits periodic pulses without any step changes. Accessibility analysis shows that the maximum radial distance from the end effector to the base is approximately 0.8 m, which is significantly less than the working radius of 2.05 m. All trajectory points are within the accessible space, the Jacobian matrix exhibits a well-conditioned state, and no singular configurations occur.

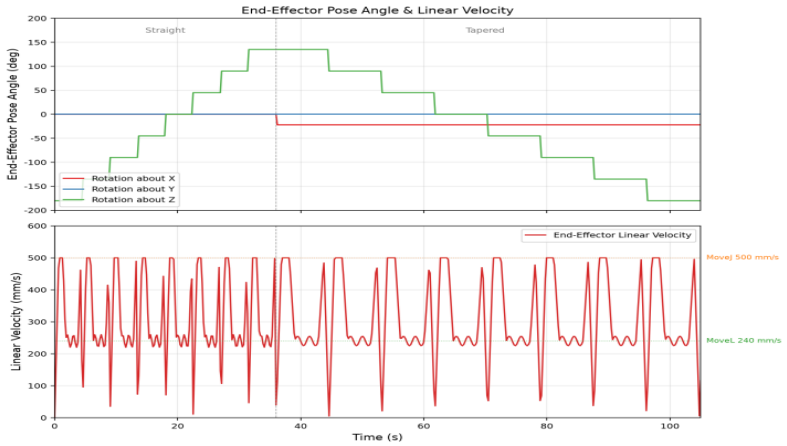


Figure 13: Graph of End-Position Angles versus Linear Velocity

Simulation results show that, under extreme operating conditions, the minimum safe clearance between the cleaning rod and the hole edge is 40 mm, and the contact clearance between the scraper and the hole wall is 0-2 mm; the system exhibits no static interference or dynamic collisions. Time measurements show that the net cleaning times for the straight and inclined sections of a single borehole are 36 s and 69 s, respectively. After accounting for auxiliary actions such as lid removal and rapid tool-change operations, the total cycle time for a single borehole is 165 s, which is less than the 180-s coal-charging cycle of the charging car for each port, demonstrating the engineering feasibility of completing the cleaning process within the coal-charging interval.

VI. CONCLUSIONS

To cope with the complex geometric features of the straight section and inverted-funnel-shaped inclined section of the coal-charging port, an automatic cleaning system was designed featuring a 310S stainless-steel cleaning rod mounted onto the end-effector of a six-axis robot. Equipped with an air-curtain structure at spray nozzles to isolate high-temperature thermal radiation, this system solved the challenge of high-temperature cleaning in confined spaces. Motion-planning simulations based on RobotStudio indicate that by adopting the alternating MoveJ/MoveL strategy and the SingArea\Wrist flexible-posture instruction, the angular displacements of all robot joints remain within permissible limits, with no singular configurations or collisions, thereby validating the rationality of the system's kinematic design. The system's net cycle time for cleaning a single port is approximately 105 s, and the complete operation cycle is 165 s, meeting the synchronization requirements for the coke oven's 180-s coal-charging cycle. This study provides a theoretical basis and engineering reference for the automation of graphite cleaning in coke oven coal-charging ports.

References

1. Ma S Y. Analysis of the Causes of Graphite Deposition in Coke Oven Carbonization Chambers and Countermeasures [J]. China Metallurgical Bulletin, 2018(05): 218-219.
2. Wang J, Xu Q, Xu J. Analysis of the Causes of Rapid Graphite Growth in 7-meter Coke Ovens and Remedial Measures [J]. Baogang Science and Technology, 2015, 41(06): 6-9.
3. Yan T J, Zhang L Y, Yang F, et al. Analysis of the Causes of Bridge Pipe Rupture in WISCO's 7.63-meter Coke Oven and Its Improvement and Repair [J]. Fuel and Chemical Industry, 2020, 51(01): 11-13,15.
4. Zhang Z Q. Mechanical Method for Cleaning Graphite from the Top of the Carbonization Chamber [J]. Fuels and Chemical Industry, 1998(04): 194.
5. Liu J C, Guo F G, Hu Z N, et al. A Graphite Cleaning Device for Coke Oven Taps [P]. Henan Province: CN202022575227.2, 2021-06-25.
6. Chen H, Yang L, Peng Z H, et al. Graphite Cleaning Device for Coke Oven Riser Tubes and Its Cleaning Method [P]. Sichuan Province: CN201310243219.X, 2015-06-03.
7. Zhong J Y, Chen B S, He F, et al. A Cleaning Rod Device for Coke Oven Charging Ports [P]. Zhejiang Province: CN202123177160.8, 2022-05-24.
8. Pei M D, Li G P, Fan X Z. High-Temperature Oxidation Behavior of 310S Stainless Steel [J]. China Metallurgy, 2016, 26(02): 31-34.
9. KACZMAREK W, BORYS S, BOCHOMULSKI M. Integration of a PLC Controller with an Industrial Robot Using the PROFIBUS-DP Protocol at a Palletizing Station [J]. PRZEGLĄD MECHANICZNY, 2019, 1(7-8): 26-29.

Funding: College Students' Innovation and Entrepreneurship Training Program (Grant No. S202612036021)